

UNCLASSIFIED

AD NUMBER
AD093306
NEW LIMITATION CHANGE
TO Approved for public release, distribution unlimited
FROM Distribution authorized to U.S. Gov't. agencies and their contractors; Administrative/Operational Use; MAR 1956. Other requests shall be referred to Office of Naval Research, One Liberty Center, 875 North Randolph Street, Arlington, VA 22203-1995.
AUTHORITY
onr ltr 9 nov 1977

THIS PAGE IS UNCLASSIFIED

UNCLASSIFIED

AD93306

Armed Services Technical Information Agency

Reproduced by

DOCUMENT SERVICE CENTER

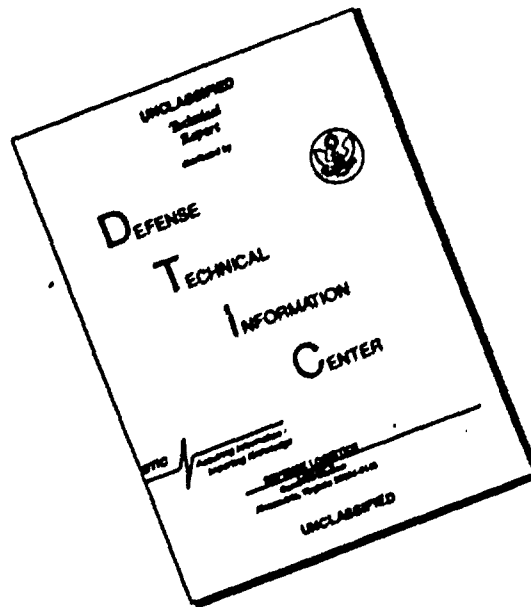
KNOTT BUILDING, DAYTON, 2, OHIO

This document is the property of the United States Government. It is furnished for the duration of the contract and shall be returned when no longer required, or upon recall by ASTIA to the following address: Armed Services Technical Information Agency, Document Service Center, Knott Building, Dayton 2, Ohio.

NOTICE: WHEN GOVERNMENT OR OTHER DRAWINGS, SPECIFICATIONS OR OTHER DATA ARE USED FOR ANY PURPOSE OTHER THAN IN CONNECTION WITH A DEFINITELY RELATED GOVERNMENT PROCUREMENT OPERATION, THE U. S. GOVERNMENT THEREBY INCURS NO RESPONSIBILITY, NOR ANY OBLIGATION WHATSOEVER; AND THE FACT THAT THE GOVERNMENT MAY HAVE FORMULATED, FURNISHED, OR IN ANY WAY SUPPLIED THE SAID DRAWINGS, SPECIFICATIONS, OR OTHER DATA IS NOT TO BE REGARDED BY IMPLICATION OR OTHERWISE AS IN ANY MANNER LICENSING THE HOLDER OR ANY OTHER PERSON OR CORPORATION, OR CONVEYING ANY RIGHTS OR PERMISSION TO MANUFACTURE, USE OR SELL ANY PATENTED INVENTION THAT MAY IN ANY WAY BE RELATED THERETO.

UNCLASSIFIED

DISCLAIMER NOTICE



**THIS DOCUMENT IS BEST
QUALITY AVAILABLE. THE COPY
FURNISHED TO DTIC CONTAINED
A SIGNIFICANT NUMBER OF
PAGES WHICH DO NOT
REPRODUCE LEGIBLY.**

This Document Contains
Missing Page/s That Are
Unavailable In The
Original Document

OR are
Blank pgs.
that have
Been Removed

**BEST
AVAILABLE COPY**

New York University
College of Engineering Research Division
University Heights
New York 53, New York

AD No. 93306
ASTIA FILE COPY

A COMPARISON OF RELATIVE VORTICITIES
COMPUTED FROM GEOSTROPHIC AND OBSERVED WINDS

By

Roy E. Peterson

FC

Technical Paper No. 5
Project SCUD
Contract No. Nonr-285(09)



Sponsored by
The Office of Naval Research

Department of Meteorology and Oceanography
March 1956

NEW YORK UNIVERSITY
COLLEGE OF ENGINEERING
RESEARCH DIVISION

A COMPARISON OF RELATIVE VORTICITIES
COMPUTED FROM GEOSTROPHIC AND OBSERVED WINDS

By

Roy E. Peterson

Technical Paper No. 5
Project SCUD
Contract No. Nonr-285(09)

Sponsored by

The Office of Naval Research

Reproduction in whole or in part is permitted for any
purpose of the United States Government.

Department of Meteorology and Oceanography

March 1956

TABLE OF CONTENTS

	Page
Abstract	v
Introduction	1
Study I	8
1. Methods	8
2. Data	18
3. Statistics	19
4. Conclusions	24
Study II	27
1. Methods	27
2. Data	29
3. Statistics	30
A. The relationship between \sum_{g6} and \sum_{o6}	30
B. The relationship between \sum_{g6} and \sum_{g3}	35
4. Discussion of errors and unrepresentativeness	40
5. Conclusions	43
Acknowledgment	44
References	45

LIST OF FIGURES

	Page
Fig. 1. Radiosonde networks used for vorticity computations	9
Fig. 2. Illustration of the method of computing vorticity (Network I)	13
Fig. 3. Scatter diagram of ζ_{o6} vs. ζ_{g3} for network I	20
Fig. 4. Scatter diagram of ζ_{o6} vs. ζ_{g3} for network II	21
Fig. 5. Scatter diagram of ζ_{o6} vs. ζ_{g3} for network III	22
Fig. 6. Scatter diagram of ζ_{o6} vs. ζ_{g3} for network IV	23
Fig. 7. Network III' used for computations of 600 km geostrophic vorticity	28
Fig. 8. Scatter diagram of ζ_{o6} vs ζ_{g6} . Winter cases	31
Fig. 9. Scatter diagram of ζ_{o6} vs ζ_{g6} . Summer cases	32
Fig. 10. Scatter diagram of ζ_{g6} vs ζ_{g3} . Winter cases	36
Fig. 11. Scatter diagram of ζ_{g6} vs ζ_{g3} . Summer cases	37

LIST OF TABLES

	Page
Table 1. Networks and stations used for computations	10
Table 2. Number of cases computed	19
Table 3. Statistical summary of the comparative analysis of 300 km geostrophic vorticity (ζ_{g3}) and 600 km observed vorticity (ζ_{o6})	24
Table 4. Stations used for computing 600 km geostrophic vorticity	27
Table 5. Statistical summary of comparative analysis of 600 km geostrophic and observed vorticities	30
Table 6. 600 km geostrophic vorticities estimated from re- gression equation for various values of 600 km observed vorticity	34
Table 7. 600 km "observed" vorticities estimated from regression equation for various values of 600 km geostrophic vorticity	34
Table 8. Statistical summary of comparative analysis of 300 km and 600 km geostrophic vorticities.	35
Table 9. 600 km geostrophic vorticities estimated from regression equation for various values of 300 km geostrophic vorticity	39
Table 10. 300 km geostrophic vorticities estimated from regression equation for various values of 600 km geostrophic vorticity	39

ABSTRACT

Two objective studies are made of geostrophic relative vorticity computed from the height field and of observed relative vorticity computed from wind components at 500 mb.

In the first study an assumption was made of linear wind variation such that observed vorticity on a 600 km scale was assumed to be representative of the 300 km scale on which the geostrophic vorticity was computed. The very poor agreement of the vorticities computed by this method indicated that this assumption was erroneous.

A second study was made, therefore, of 600 km scale observed vorticity and of 300 km and 600 km scale geostrophic vorticity. The comparison of geostrophic vorticity of different scales indicated the importance of grid size in the computations. The comparison of observed and geostrophic vorticity of the same scale indicated small though significant differences.

A COMPARISON OF RELATIVE VORTICITIES COMPUTED FROM GEOSTROPHIC AND OBSERVED WINDS

I. INTRODUCTION

Within recent years the vorticity concept has come into increasingly greater use in both synoptic and dynamic meteorology. In most studies of vorticity the geostrophic approximation has been used to compute the relative vorticity from the height field of a constant pressure chart in preference to the use of the upper-air wind field. Many theoretical and practical reasons have been proposed both to justify and to qualify the use of this technique. In numerical weather prediction, for example, the use of the geostrophic assumption is advantageous, not only as a filter to remove certain undesirable wave solutions, but as a convenient means of dealing directly with functions of a scalar height field rather than reducing wind fields into the scalar magnitudes of components or making separate computations of wind shear and curvature. Recent studies of cyclogenesis (Spar, et al., 1955) have been based upon the initial determination of geostrophic vorticity before the computation of the advective and generative terms of the vorticity equation at various upper levels above regions of cyclogenesis. The use of the vorticity concept in meteorology has become so increasingly important, and the use of the geostrophic assumption is so widespread, that an estimate of the validity of the geostrophic technique is of considerable concern.

Much study has already been devoted to the deviations of the geostrophic from the observed wind, and more especially in recent years to the vorticity deviations which naturally arise from such differences. Charney (1948) laid much of the basis of current computational techniques in numerical weather prediction by reasoning on theoretical grounds that the geostrophic deviation is negligible for those primary large-scale perturbations where the mean horizontal distance between trough and wedge is of the order of 1000 km. His conclusion was based on the assumption of typical values for the orders of magnitude of the mean horizontal distance between trough and wedge, the mean vertical distance between points at which velocity components assume extreme values, the mean magnitudes of the horizontal and vertical velocity components, and the mean speed of propagation of the system. Charney was thus able to show that the horizontal acceleration of a 1000 km perturbation is one order of magnitude less than that of the horizontal Coriolis force.

Among the early synoptic investigations of geostrophic wind deviations was that by Houghton and Austin (1946), who studied the deviations of the geostrophic wind at 10,000 feet. They measured the geostrophic wind components from the spacing between isobars and obtained the actual wind components from PIBAL and RAWIN observations. By then subtracting the geostrophic from the observed wind component, they obtained the geostrophic deviations, u' and v' . For 619 cases they computed a mean absolute value of u' and v' as 7.0 mph, compared to mean absolute values

of the geostrophic components, $U_{gs} = 18.7$ mph and $V_{gs} = 12.7$ mph. The magnitude of the mean vector difference between the actual and the geostrophic wind was 10.8 mph. The deviations u' and v' were accepted as real since their isopleths formed systematic patterns.

Neiburger et al. (1948) performed geostrophic and gradient wind computations for all wind-reporting stations on two 700-mb charts (135 cases in all). A variability of about 25 percent was found in the computations made by different individuals in the same cases. The computed geostrophic wind speeds differed by about 35 percent from the observed wind speeds. A study of deviations as a function of curvature produced no significant correlation, although computed winds were predominantly greater than the observed when the contour curvature was anticyclonic or neutral, and more evenly distributed between greater and smaller values when the curvature was cyclonic.

Godson (1950) studied 618 cases at 10,000 feet for a 3-day sequence over the North American continent. He computed a mean absolute angle of $14.4^\circ \pm 0.7^\circ$ between the reported and the geostrophic winds. The mean absolute deviation of the speeds was approximately 7 mph. For latitudes north of 30° N and for a range of geostrophic wind speed between 20 and 45 mph, the difference between observed and geostrophic wind is approximately 20 percent of the true wind speed.

Reed (1951) considered the effect of using geostrophic winds for vorticity computations at 4 and 10 thousand feet. He computed relative

vorticity, ζ , from the following equation, which expresses the shear and curvature terms in natural coordinates:

$$\zeta = -\partial v / \partial n + v \partial \alpha / \partial s ,$$

where v = velocity of the wind, n = direction normal to the streamlines, α = wind direction in radian measure, and s = distance in the streamline direction. Graphical addition was used to add the separate shear and curvature components. From the results of his study, Reed concluded that geostrophic vorticity may be substituted for the actual whenever the spacing and curvature of the contours can be determined with a minimum of ambiguity.

Newton (1954) studied the effect of contour analysis on the computed vorticity field. Geostrophic vorticity calculations were found to be very sensitive to details of analysis since second-order differentials of the height field are used. He suggested that arbitrary variations in the vorticity field be minimized by smoothing. Newton also pointed out that the error in computed geostrophic wind varies inversely with the distance between stations, for a given height error.

Hovmöller (1952) considered the effect of temperature measurement errors in the following manner: if we have two stations, A and B, the relative error of the geostrophic wind perpendicular to AB can be shown to be

$$\frac{(\Delta V_g)_n}{(V_g)_n} \approx \frac{(\Delta T_A - \Delta T_B) Z_A}{Z_A - Z_B} \frac{1}{T_A}$$

where $(\Delta T_A - \Delta T_B)$ is the difference of the mean temperature errors of the station soundings for the entire layer below the level considered. At 500 mb, if we assume as typical values: $Z_A = 5700$ m, $T_A = 250^\circ\text{A}$, $(Z_A - Z_B) = 50$ m, and $(\Delta T_A - \Delta T_B) = 1^\circ\text{A}$,

$$\frac{(\Delta V_g)_n}{(V_g)_n} \approx 45\%$$

On the basis of these considerations Hovmöller declared that it was inadvisable to use unsmoothed height values for computing geostrophic vorticity; in fact, he stated that in many cases at 500 mb the observed wind normally may be a better approximation to the geostrophic wind than the value derived from the height field. He concluded by stating a preference for the following method to compute relative vorticity from the observed winds

$$\zeta = \Delta v / \Delta x - \Delta u / \Delta y$$

where Δu and Δv are finite differences of the wind velocity components as measured along intervals Δx and Δy which are centered at the origin of a Cartesian coordinate system.

Aubert (1953) showed that the use of the geostrophic wind approximation in relative vorticity calculations at 500 mb is equivalent to using analyzed wind fields having a standard error of 9 mps (these results were based on calculations made over 5-degree "squares"). Since this is considerably larger than the value of the standard wind

error obtained by Rapp (1952), he concluded that the relative vorticity can best be obtained from observed winds. Aubert analyzed 500 mb maps for four synoptic periods, analyzed the wind fields by the Bjerknes isogon-isotach technique, the height contours by the usual technique of subjective interpolation, and in each analysis made visual reference to the other. The geostrophic wind at the grid points was computed over a length increment of 2.5 degrees of latitude. The relative vorticity was then computed from the wind values as the average circulation per unit area over 5 and 10 degree "squares".

For the 5 degree "square", Aubert obtained a linear correlation coefficient $r = 0.529$ for 242 cases, a standard deviation of relative vorticity of observed wind, $\sigma = 3.81 \times 10^{-5} \text{ sec}^{-1}$, a standard deviation of relative vorticity of geostrophic wind, $\sigma_g = 4.59 \times 10^{-5} \text{ sec}^{-1}$, and a standard error of estimating the relative vorticity of the observed wind from that of the geostrophic wind, $s = 3.23 \times 10^{-5} \text{ sec}^{-1}$. For a 10-degree grid, Aubert obtained these values: $r = 0.773$, $\sigma = 2.80 \times 10^{-5} \text{ sec}^{-1}$, $\sigma_g = 2.24 \times 10^{-5} \text{ sec}^{-1}$, and $s = 1.78 \times 10^{-5} \text{ sec}^{-1}$. The latter results show the effect of greater space smoothing obtained by quadrupling the area over which the circulation integral was evaluated.

In connection with a vorticity study of east coast cyclogenesis, Spar et al. (1955) compared vorticity values computed by the wind component method with those obtained by the geostrophic method. 500 mb data for three upper-air observation times are used, and vorticity

values on a 300 km scale were computed from analyzed charts of height contours and wind components. A comparison of approximately 225 absolute vorticity values revealed a close agreement between the means, only slight differences between respective maxima and minima, and a close similarity between analyzed vorticity patterns. The contour analysis was, however, drawn to fit the wind data so that the two computations were not based upon independent data.

A serious criticism of many previous studies of geostrophic vorticity deviations is their basis upon synoptically dependent analyses of winds and contours, as a result of which both real and unreal differences are smoothed out. The great advantage of a smoothing technique is the correction applied to erroneous and unrepresentative observations; the disadvantage, however, is the large degree of subjectivity involved in the many decisions of accuracy and representativeness which are necessarily made in the analysis of a constant pressure chart. Miller (1947) remarked that when the number of pressure and wind data is not infinite, it is always possible to construct isobars such that every observed wind is equal to the geostrophic wind. Since such a wide degree of discretion is available to the analyst, the degree of correspondence between geostrophic and observed winds and velocities is as variable as the ability, experience and synoptic idiosyncrasy of the individual analyst. In addition, the scale of the analysis is rather variable: where the data are dense, the analysis is on a smaller scale than where sparser data necessitate a

greater degree of interpolation. Also, studies based upon the small sample of a few synoptic situations may lack generality in their results. All these factors combine to subject synoptic studies of vorticity to a large indeterminate degree of variance.

It is proposed, therefore, that in this study objective methods of vorticity computation be used to test the hypothesis that a significant difference exists between geostrophic and observed vorticity at 500 mb. Such a method, though sensitive to observational error and unrepresentativeness, has the advantage of greater sensitivity to real differences. Estimates of observational error and of unrepresentativeness can be made. The ultimate question is whether a valid estimate of real differences in the two vorticities can be detected above this background level of error.

STUDY I

1. Methods

In Study I four networks of five rawinsonde stations each were used for objective calculations at 500 mb of geostrophic vorticity from the reported heights and of observed vorticity from the components of the reported winds. The networks are shown in figure 1 and the individual stations are listed in Table 1.

A 300 km scale was initially chosen for this study, on the basis of its rather widespread use. Since the geostrophic vorticity is computed from the second derivative of the height field and the observed vorticity

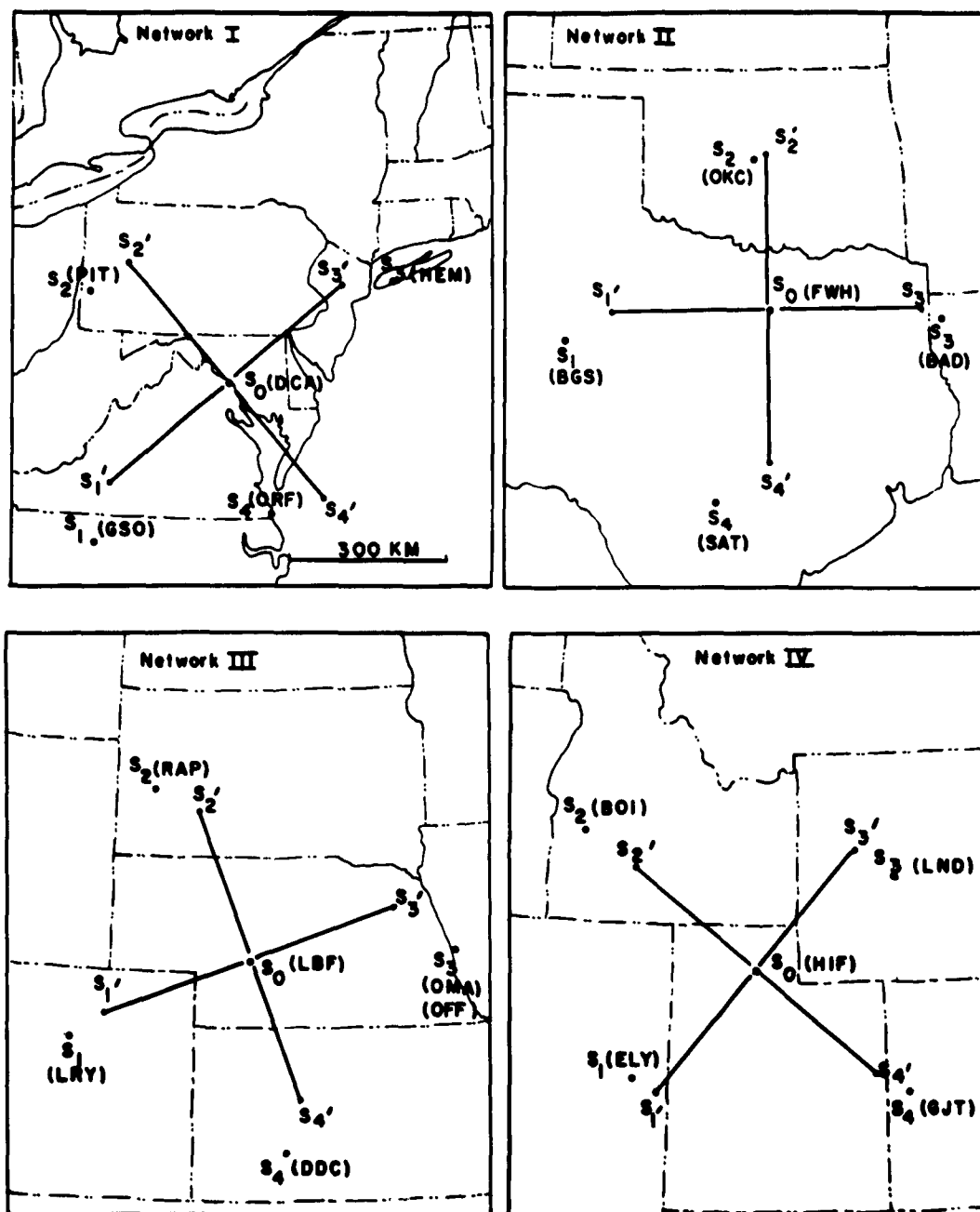


FIG.1. Radioisotope networks used for vorticity computations.

Table 1. Networks and stations used for computations.

	<u>Network I</u>	<u>Network II</u>	<u>Network III</u>	<u>Network IV</u>
S_0 (center)	Washington (DCA)	Fort Worth (FWH)	North Platte (LBF)	Ogden (HIF)
S_1 ("west")	Greensboro (GSO)	Big Springs (BGS)	Denver (LRY)	Ely (ELY)
S_2 ("north")	Pittsburgh (PIT)	Oklahoma City (OKC)	Rapid City (RAP)	Boise (BOI)
S_3 ("east")	Hempstead (HEM)	Shreveport (BAD)	Omaha (OMA, OFF)	Lander (LND)
S_4 ("south")	Norfolk (ORF)	San Antonio (SAT)	Dodge City (DDC)	Grand Junction (GJT)

from the first derivative of the wind field, the grid size used for determining observed vorticity should be one-half the size used for computing geostrophic vorticity. It was not possible, however, to locate such a smaller network of wind reporting stations within the larger network of height reporting stations. It was assumed, therefore, that the magnitude of the wind components varied linearly between the central station and each of the outer stations, an assumption which states in effect that observed vorticity of a 600 km scale is equivalent to that of a 300 km scale. This assumption of linear wind change is commonly used to interpolate between data on synoptic charts and is the best estimate of wind change that can usually be made (Rapp, 1952),

Only those networks were chosen for this study whose outside stations were approximately 300 km from the central station and so

located that perpendicular axes through the central station could be drawn close to each. Only the grid axes of network II could be oriented north-south; the axes of the other networks were rotated so as to minimize the mean distance of the outside stations from the axes. A linear interpolation process was then used to transform station values into grid values by the application of small corrections. As an example of how this procedure was applied, we shall only consider network I, since the other networks were treated similarly.

A diagram of network I is shown in figure 2. The axes of the grid were rotated 40 degrees counterclockwise, to satisfy the condition that the outside stations be the shortest mean distance from the axes. Next, the transformation of station to grid values was developed in terms of a general scalar quantity S to be later applied specifically to the heights and the wind components. To obtain grid value S_1' , for example, we first interpolate the value for the intersection of the line $\overline{S_1 S_2}$ with the X' axis. The interpolated value, S_1^* , can be expressed as

$$S_1^* = S_2 + \frac{\overline{S_1^* S_1}}{\overline{S_1 S_2}} (S_2 - S_1)$$

If we now substitute the value of $\overline{S_1^* S_1} / \overline{S_1 S_2}$,

$$S_1^* = S_1 + .167(S_2 - S_1)$$

or

$$S_1^* = .833 S_1 + .167 S_2 .$$

The value of S_1' can now be obtained by interpolation between S_1^* and S_0 as follows:

$$S_1' = S_1^* - \frac{\overline{S_1^* S_1'}}{\overline{S_1^* S_0}} (S_0 - S_1^*) .$$

If we now substitute the value of $\overline{S_1^* S_1'} / \overline{S_1^* S_0}$,

$$S_1' = S_1^* - .104(S_0 - S_1^*) ,$$

or

$$S_1' = 1.104 S_1^* - .104 S_0 .$$

If we substitute the value derived for S_1^* ,

$$S_1' = .92 S_1 + .18 S_2 - .10 S_0 .$$

In a similar manner the values of S_2' , S_3' and S_4' can be obtained. The procedure can be summarized as follows:

1. Interpolate linearly to obtain the value at the intersection of an axis with the line joining two stations values.
2. When the intersection is outside the grid, interpolate between the intersection and the central station to obtain the value at the grid point.
3. When the intersection is within the grid, extrapolate the gradient between the intersection and the central station to obtain the value at the grid point.

The following is a summary of the relationships thus derived for the four networks:

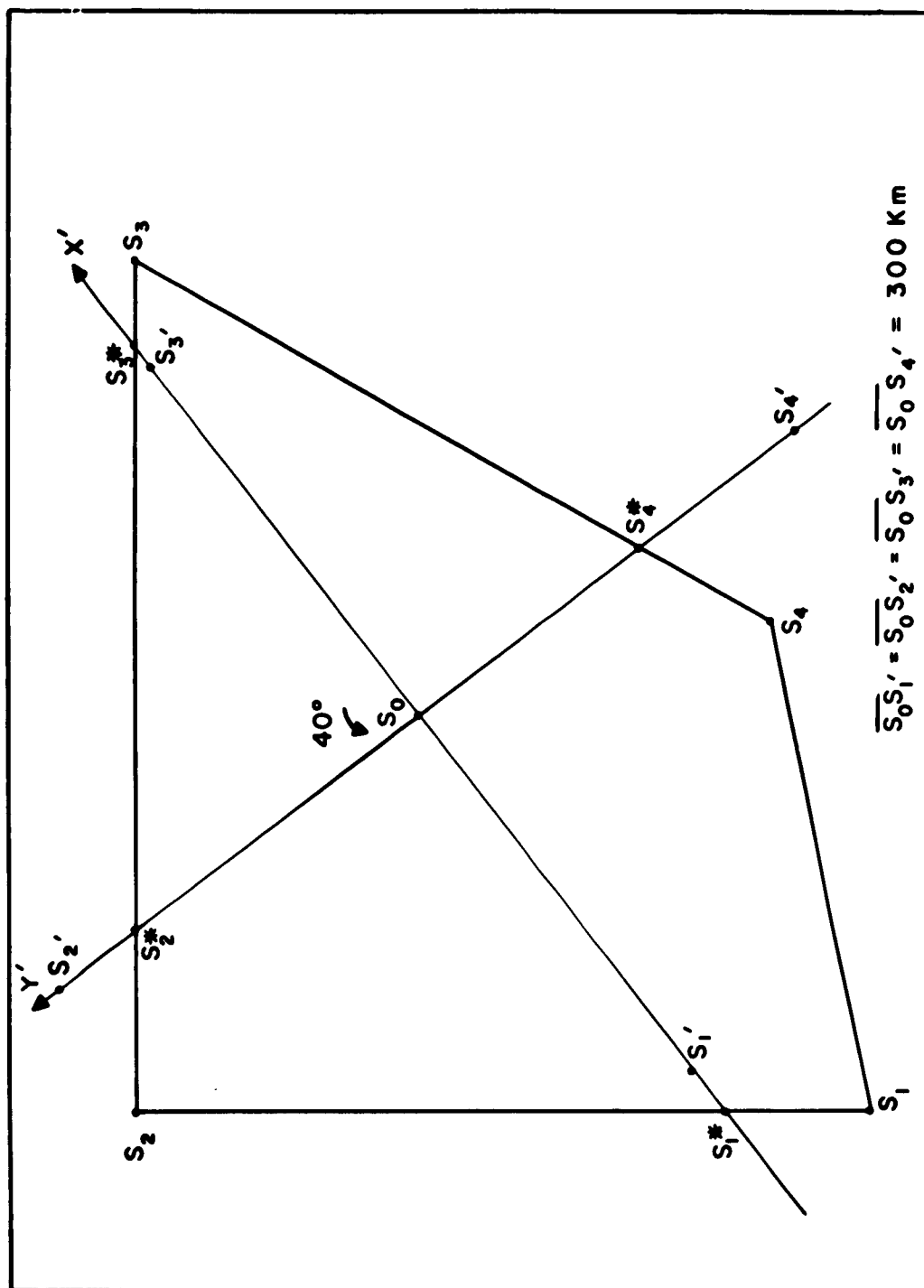


FIG. 2. Illustration of the method of computing vorticity. (Network I)

Network I

$$S_1' = .92 S_1 + .18 S_2 - .10 S_0$$

$$S_2' = .60 S_2 + .18 S_3 + .22 S_0$$

$$S_3' = .96 S_3 + .09 S_2 - .05 S_0$$

$$S_4' = 1.00 S_4 - .22 S_1 + .22 S_0$$

Network II

$$S_1' = .93 S_1 + .16 S_2 - .09 S_0$$

$$S_2' = .83 S_2 + .06 S_3 + .11 S_0$$

$$S_3' = .99 S_3 + .06 S_2 - .05 S_0$$

$$S_4' = .70 S_4 + .23 S_3 + .07 S_0$$

Network III

$$S_1' = 1.11 S_1 + .06 S_2 - .17 S_0$$

$$S_2' = .86 S_2 + .14 S_3$$

$$S_3' = .69 S_3 + .20 S_2 + .11 S_0$$

$$S_4' = .96 S_4 + .14 S_3 - .10 S_0$$

Network IV

$$S_1' = .76 S_1 + .11 S_4 + .13 S_0$$

$$S_2' = .71 S_2 + .29 S_0$$

$$S_3' = .68 S_3 + .14 S_2 + .18 S_0$$

$$S_4' = 1.08 S_4 + .05 S_1 - .13 S_0$$

The observed relative vorticity will be computed from the finite difference form of the equation

$$\zeta = \frac{\partial v}{\partial x} - \frac{\partial u}{\partial y} \quad (1)$$

Since $\Delta x = \Delta y = 600$ km, and the wind components are expressed in knots,

$$\begin{aligned} \zeta_{06} &= \frac{[(v_3' - v_1') - (u_2' - u_4')]}{6 \times 10^{-5} \text{ m}} \text{ knots} \times \frac{.515 \text{ m sec}^{-1}}{\text{knot}} \\ &= .086 (v_3' - v_1' - u_2' + u_4') \times 10^{-5} \text{ sec}^{-1} . \end{aligned}$$

If we now apply to network I, for example, the relationship for interpolating grid values from station values,

$$\begin{aligned} v_3' &= .96 v_3 + .09 v_2 - .05 v_0 \\ v_1' &= .92 v_1 + .18 v_2 - .10 v_0 \\ u_2' &= .60 u_2 + .18 u_3 + .22 u_0 \\ u_4' &= 1.00 u_4 - .22 u_1 + .22 u_0 . \end{aligned}$$

It may be noted that the interpolation process introduces wind components from the central station into the calculation. By substituting the values given above into the equation ζ_{06} , we obtain as the final expression for network I,

$$\begin{aligned} \zeta_{06I} &= .086 (.96 v_3 - .92 v_1 - .09 v_2 + .05 v_0 - .60 u_2 \\ &\quad + 1.00 u_4 - .22 u_1 - .18 u_3) \times 10^{-5} \text{ sec}^{-1} . \end{aligned}$$

Similarly, we obtain for the other networks

$$\zeta_{06II} = .086 (.99 v_3 - .93 v_1 - .10 v_2 + .04 v_0 - .83 u_2 \\ + .70 u_4 + .17 u_3 - .04 u_0) \times 10^{-5} \text{ sec}^{-1} .$$

$$\zeta_{06III} = .086 (.69 v_3 - 1.11 v_1 + .14 v_2 + .28 v_0 - .86 u_2 \\ + .96 u_4 - .10 u_0) \times 10^{-5} \text{ sec}^{-1} .$$

$$\zeta_{06IV} = .086 (.68 v_3 - .76 v_1 + .14 v_2 - .11 v_4 + .05 v_0 \\ - .71 u_2 + 1.08 u_4 + .05 u_1 - .42 u_0) \times 10^{-5} \text{ sec}^{-1} .$$

The equation for computing geostrophic relative vorticity can be derived from the basic equation (1). The geostrophic equations for the wind components, u and v , are

$$u = -g_0 / f \partial h / \partial y \quad (2)$$

and

$$v = g_0 / f \partial h / \partial x$$

where g_0 is the standard acceleration of gravity, f is the Coriolis parameter, and h is the geopotential height of the isobaric surface. If we substitute u and v in the vorticity equation

$$\zeta_g = \frac{\partial}{\partial x} \left(\frac{g_0}{f} \frac{\partial h}{\partial x} \right) + \frac{\partial}{\partial y} \left(\frac{g_0}{f} \frac{\partial h}{\partial y} \right) .$$

Since $\partial f / \partial x = 0$ and $\partial f / \partial y$ is here considered negligible,

$$\zeta_g = \frac{g_0}{f} \left(\frac{\partial^2 h}{\partial x^2} + \frac{\partial^2 h}{\partial y^2} \right) .$$

We can approximate $(\partial^2 h / \partial x^2 + \partial^2 h / \partial y^2)$, however, by the expression $(h_1 + h_2 + h_3 + h_4 - 4h_0) / L^2$, where $L = \Delta x / 2 = \Delta y / 2$. Thus

$$\zeta_g = \frac{g_0}{f} (h_1 + h_2 + h_3 + h_4 - 4h_0) / L^2 \quad (3)$$

Since $L = 300 \times 10^3 \text{ m}$

$$g_0 = 9.81 \text{ m sec}^{-2}$$

and $1 \text{ ft} = .305 \text{ m}$,

$$\zeta_{g3} = \frac{.332}{f} (h_1' + h_2' + h_3' + h_4' - 4h_0) \times 10^{-9} \text{ sec}^{-1},$$

where h' denotes the interpolated geopotential height of the isobaric surface in tens of feet.

If we consider, for example, network I where the latitude of the central station is 38.8° N and $f = .914 \times 10^{-4} \text{ sec}^{-1}$.

$$\zeta_{g3I} = .363 (h_1' + h_2' + h_3' + h_4' - 4h_0) \times 10^{-5} \text{ sec}^{-1}.$$

If we express the grid values in terms of the station values of height, as derived previously,

$$h_1' = .92h_1 + .18h_2 - .10h_0$$

$$h_2' = .60h_2 + .18h_3 + .22h_0$$

$$h_3' = .96h_3 + .09h_2 - .05h_0$$

$$h_4' = 1.00h_4 - .22h_1 + .22h_0$$

Upon substituting these values,

$$\zeta_{g3I} = .363 (0.70h_1 + 0.87h_2 + 1.14h_3 + 1.00h_4 - 3.71h_0) \times 10^{-5} \text{ sec}^{-1}.$$

Similarly we obtain for the other networks,

$$\zeta_{g3II} = .421 (0.93h_1 + 1.05h_2 + 1.28h_3 + 0.70h_4 - 3.96h_0) \times 10^{-5} \text{ sec}^{-1}.$$

$$\zeta_{g3III} = .347 (1.11h_1 + 1.12h_2 + 0.97h_3 + 0.96h_4 - 4.16h_0) \times 10^{-5} \text{ sec}^{-1}.$$

$$\zeta_{g3IV} = .346 (0.81h_1 + 0.85h_2 + 0.68h_3 + 1.19h_4 - 3.53h_0) \times 10^{-5} \text{ sec}^{-1}.$$

Throughout the remainder of this paper all vorticity values will be understood to be in units of 10^{-5} sec^{-1} .

2. Data

The original plan of Study I was to compute geostrophic and observed vorticity from 500 mb data for the entire year 1953. The preliminary results were such, however, that this study was limited to 0300Z data for the period January-June 1953. The data were obtained from the Daily Upper Air Bulletins, original teletype data, and from microfilmed copies of WBAN Form 33, Summary of Constant Pressure Data (obtained from the National Weather Records Center, USWB). WBAN 33 would have been used exclusively in this study, but the coding of wind directions to 16 points on this form made such data virtually unusable except as a check for gross errors in the transmitted values of wind direction, which are coded to a 36-point wind scale. After conversion to appropriate units, however, such data were occasionally used to fill in gaps where the data were otherwise complete for a network.

The height values from WBAN 33, which are listed in tens of meters, were converted to units of ten feet, and these values were also used as a check on the transmitted data and to fill in occasional gaps. This checking system eliminated many errors of coding and transmission, so that the data used in the objective calculations were the best available.

The wind data were those reported for the 500 mb surface with two exceptions: for Pittsburgh, where the RAWINS are reported separately from the RAOBS, the wind was interpolated to the height of the 500 mb surface; and for Omaha, where only sparse PIBALS were available,

RAWIN data from Offutt AFB were used by interpolating the wind to the RAOB height reported by Omaha.

Since the objective system of calculation required five wind and height reports for each network, the rate of attrition was quite large. Table 2 lists the monthly totals for each network where the data were complete.

Table 2. Number of cases computed.

<u>Network</u>	<u>Jan.</u>	<u>Feb.</u>	<u>Mar.</u>	<u>Apr.</u>	<u>May</u>	<u>June</u>	<u>Total</u>
I	8	8	17	12	15	17	77
II	6	12	10	14	21	25	88
III	5	2	6	10	13	19	55
IV	6	6	12	8	3	11	46
Total	25	28	45	44	52	72	266

3. Statistics

Scatter diagrams (figs. 3, 4, 5, 6) represent graphically the relations between ζ_{06} and ζ_{g3} which were found for each network. The noteworthy features of these diagrams are the considerably greater range of values of ζ_{g3} and the weak relation between the two vorticities. Of special interest are the large negative values of geostrophic vorticity found in networks I and II, many of which exceed the value of the Coriolis parameter.

The following statistics were computed: the arithmetic means,

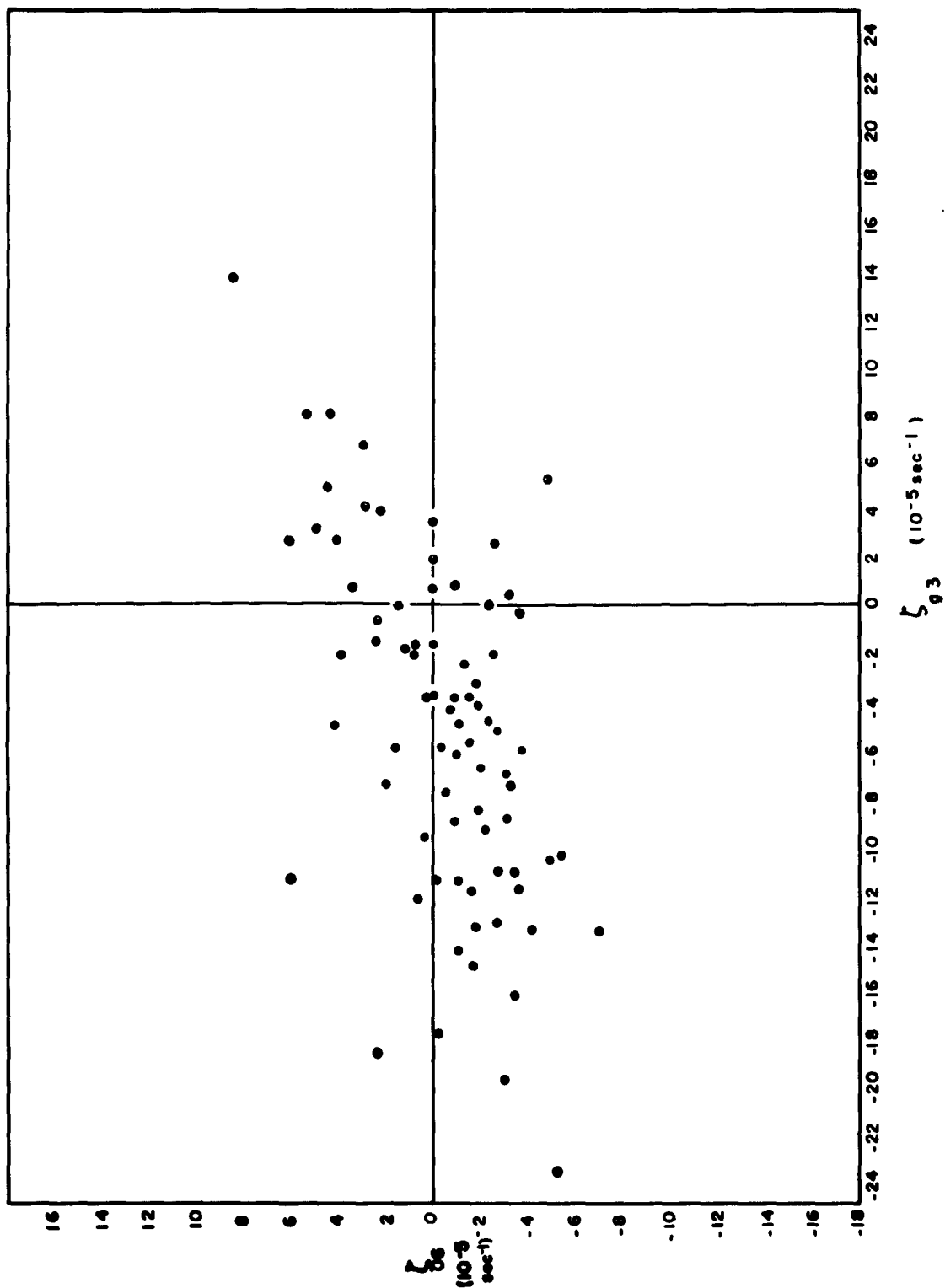


FIG. 3. Scatter diagram of L_{06} vs. L_{g3} for network I.

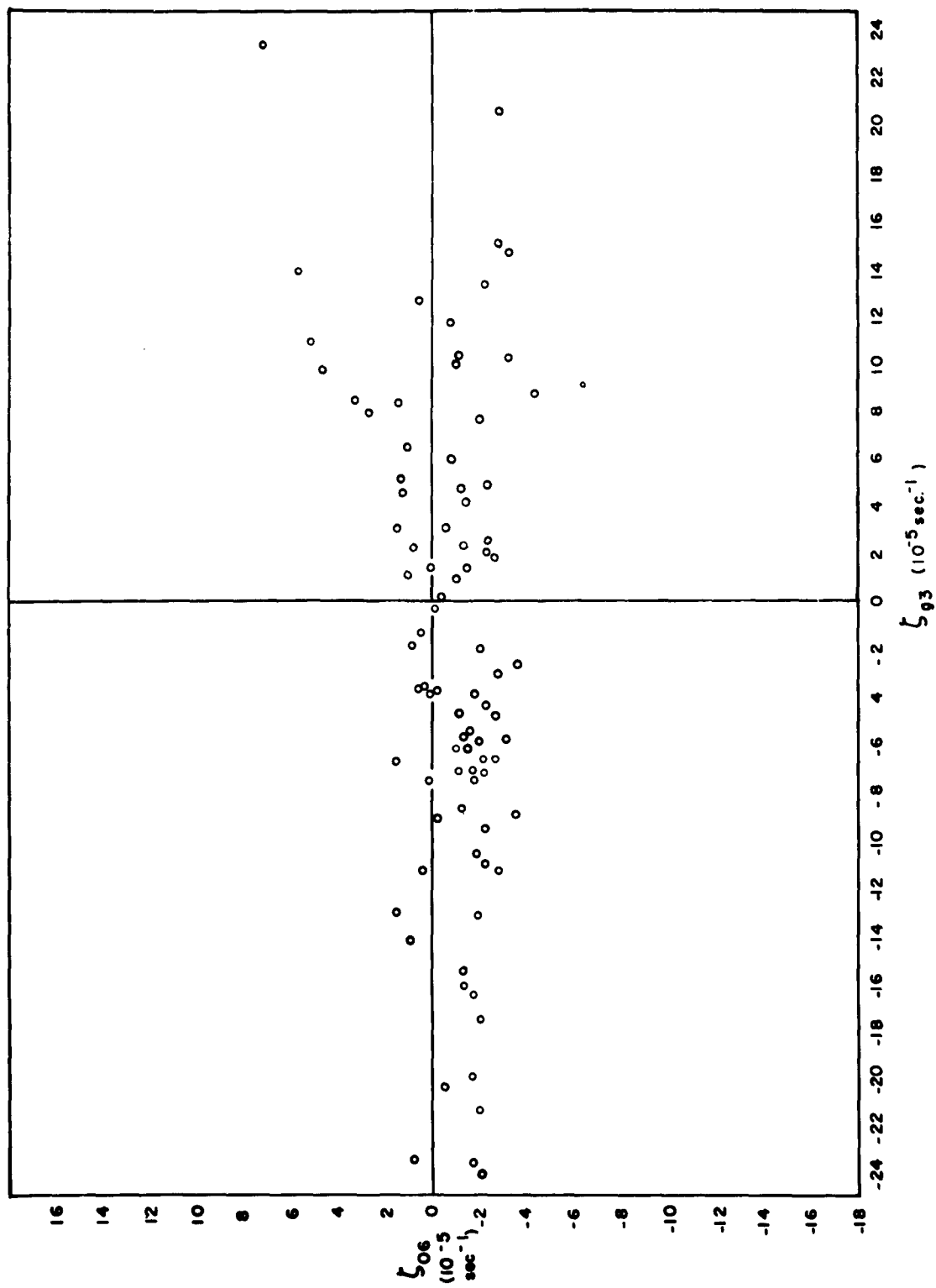


FIG. 4. Scatter diagram of L_{06} vs. L_{g3} for network II.

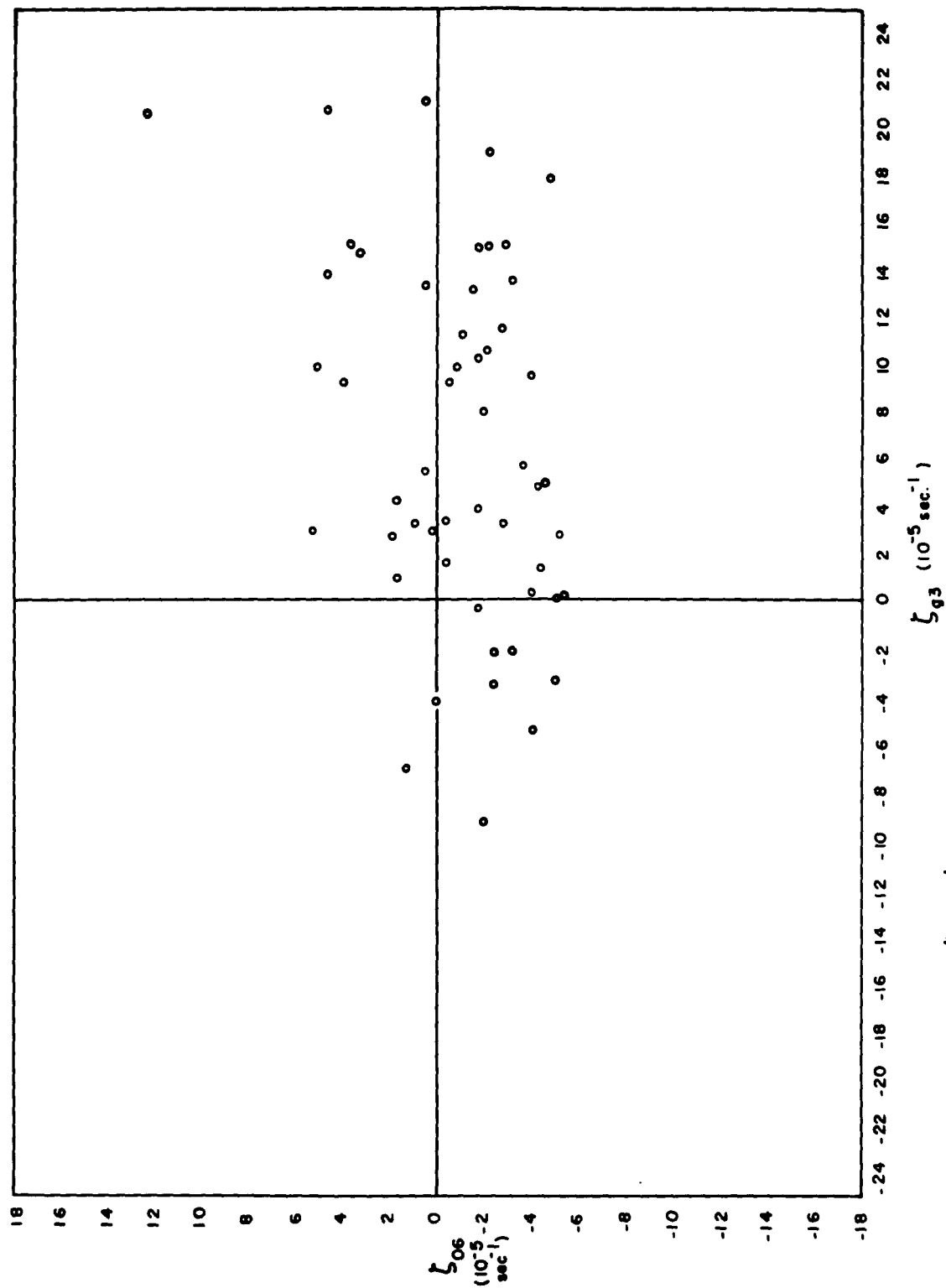


FIG. 5. Scatter diagram of L_{06} vs. L_{g3} for network III.

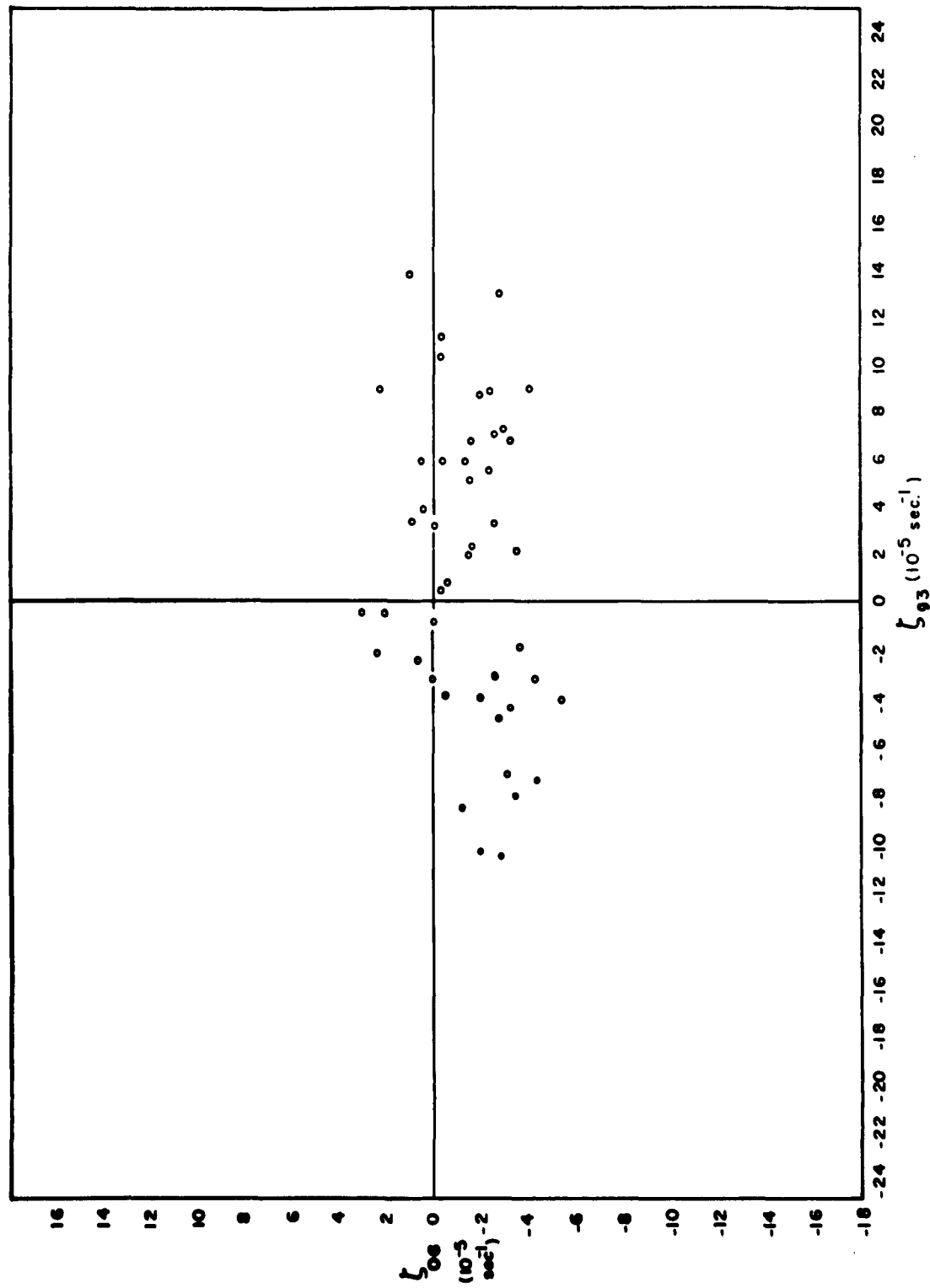


FIG. 6. Scatter diagram of ζ_{06} vs. ζ_{93} for network IV.

$\overline{\xi}_{g3}$ and $\overline{\xi}_{o6}$; the standard deviations, σ_{g3} and σ_{o6} ; and the linear correlation coefficients, r , between ξ_{g3} and ξ_{o6} for the networks individually and collectively. These values are presented in Table 3 below.

Table 3. Statistical summary of the comparative analysis of 300 km geostrophic vorticity (ξ_{g3}) and 600 km observed vorticity (ξ_{o6}).

Network	n	$\overline{\xi}_{g3}$	$\overline{\xi}_{o6}$	σ_{g3}	σ_{o6}	r
I	77	-5.13	-0.44	7.18	3.03	.540
II	88	-1.99	-0.82	10.22	2.14	.246
III	55	7.89	-0.73	9.02	3.37	.323
IV	46	1.52	-1.37	6.30	1.93	.211
Total	266	-0.25	-0.79	9.76	2.69	.270

4. Conclusions

The linear coefficients are so low as to be insignificant. The standard deviation of ξ_{g3} is, for the combined cases, more than three times larger than that of ξ_{o6} . This striking difference in the distributions of the two vorticities can be attributed to a combination of the following factors: observational errors, to which the geostrophic vorticity, computed from the second derivative of the height field, is especially sensitive due to the lack of smoothing; unrepresentativeness, to which the observed vorticity is especially vulnerable, and which can be reasonably expected to flatten out the range of values; the scale

effect, which was introduced into this study by the assumption that the wind components varied linearly from the central station to the outer stations; and finally, any real differences between the two vorticities.

Of the factors mentioned above as accounting for the large difference in the standard deviations of ξ_{g3} and ξ_{o6} , estimates of the effects of observational errors and unrepresentativeness can be made (and will be presented later in this paper). The real differences between the two vorticity distributions are most probably obscured by the systematic scale effect introduced into this study. If the assumption of linear wind variations was not valid, the original hypothesis was not subjected to a fair test. The results of this study raise, therefore, an important question as to the limitation imposed by the density of data upon the scale chosen for vorticity computations. Interpolation too far within the data network may seriously affect vorticity computations purporting to be finer than the coarseness of the data will allow. Such may be the case here, where it is assumed that the observed vorticity at a 600 km scale may be considered equivalent to that on a 300 km scale.

Landers (1955) has presented an example of the effect produced on vorticity computations by the scale of wind observations. From a large-scale analysis of synoptically reported winds at 30,000 feet, anticyclonic relative vorticity was computed over a large region, whereas from a small-scale analysis of B-29 winds at the same level for approximately

the same time, cyclonic relative vorticity was predominant over the same region. The ratio of small to large scale maximum gradients of vorticity was six to one. It would thus appear that interpolation of synoptic wind data for computing smaller-scale vorticity may be subject to large errors.

STUDY II

1. Methods

The results of the previous study indicated the probable seriousness of the assumption of linear wind variation between observing stations. It was decided, therefore, to alter the plan of study so that the effect of scale on vorticity computations could both be removed and investigated separately. A method was designed to compare 600 km geostrophic and observed vorticity, and in addition, to compare 300 km and 600 km geostrophic vorticity. A network for computing 600 km geostrophic vorticity was chosen whose central station coincided with that of network III. From these concentric networks three sets of vorticity values could be computed.

The larger network for computing 600 km geostrophic vorticity, which we shall designate as network III', is shown in figure 7. The individual stations are listed in Table 4. The axes of network III', chosen

Table 4. Stations used for computing 600 km geostrophic vorticity.

<u>Station</u>	<u>Network III'</u>
S_0 (center)	North Platte (LBF)
S_1 ("west")	Lander (LND)
S_2 ("north")	Bismarck (BIS)
S_3 ("east")	Columbia (CBI)
S_4 ("south")	Amarillo (AMA)

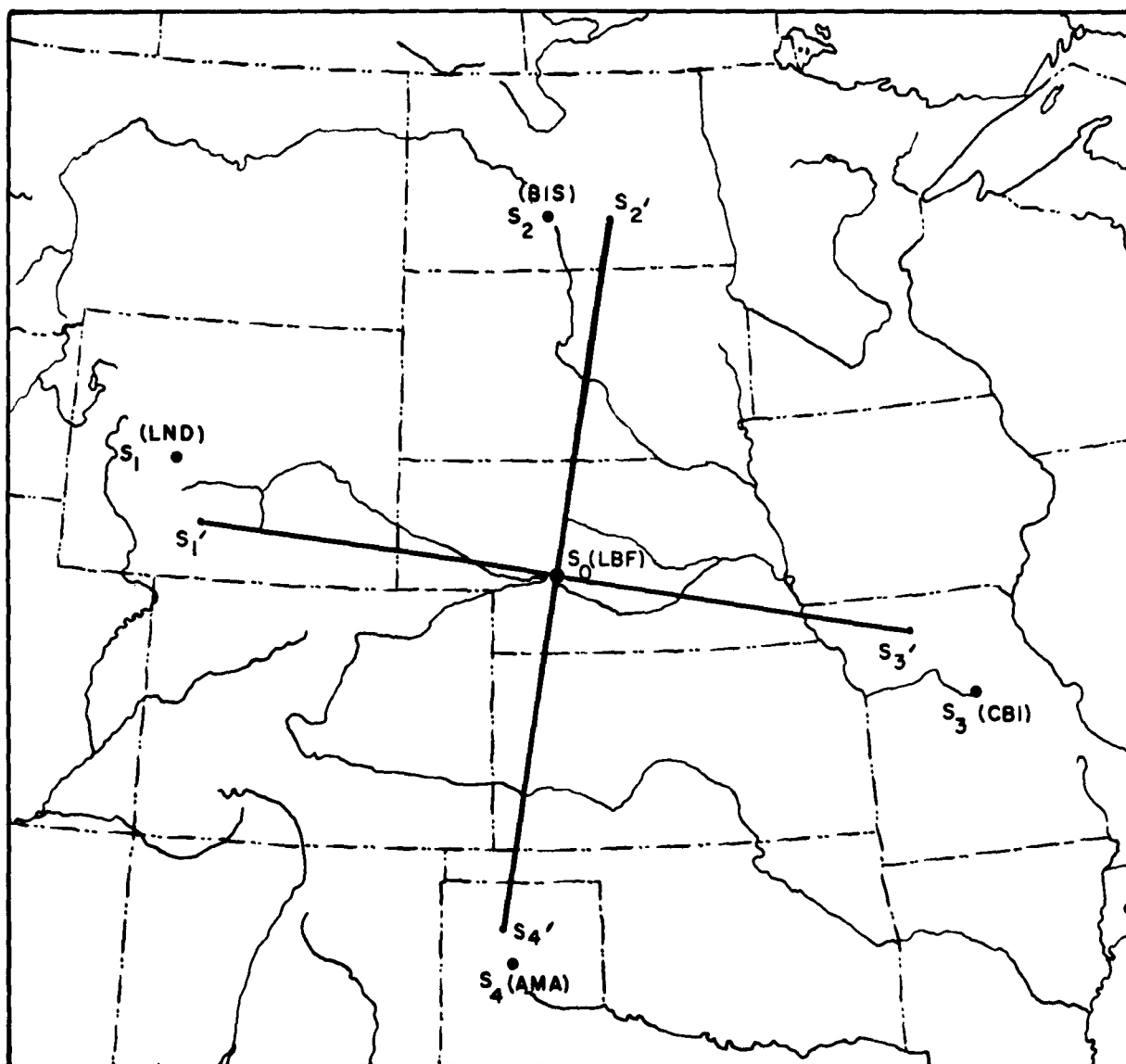


FIG.7. Network III' used for computations of 600km geostrophic vorticity.

to minimize the interpolation necessary for computing grid values of height from station values was placed clockwise from the axes of network III.

The relationships previously derived in Study I for ζ_{o6III} and ζ_{g3III} were again applied to this study; the same methods used in their derivation were applied to the larger network and the following expression thus obtained for computing the 600 km geostrophic vorticity:

$$\zeta_{g6III} = 0.087 (0.86 h_1 + 0.80 h_2 + 1.08 h_3 + 1.13 h_4 - 3.87 h_0) \times 10^{-5} \text{ sec}^{-1}.$$

Three vorticity values were then computed: ζ_{g3} , ζ_{o6} , and ζ_{g6} (the subscript denoting the network is no longer necessary). Only those cases were selected where all three values could be obtained, so that the comparison between ζ_{o6} and ζ_{g6} and that between ζ_{g3} and ζ_{g6} were based upon the same observations.

2. Data

A total of 385 cases were selected from 0300Z and 1500Z upper air data for the year 1953. The following is the monthly distribution of cases for the months January to December, respectively: 18, 14, 15, 36, 27, 39, 47, 47, 44, 40, 31, 27. It is apparent that the summer months have a larger number of cases than the winter months. In an attempt to eliminate some of the bias resulting from the unequal seasonal distribution, the cases were divided into two groups; the "winter" group of months were Jan., Feb., Mar., April, Nov., and Dec., and the "summer" group of the months were May, June, July, Aug., Sept., and Oct. The winter cases total 141; the summer cases 244.

3. Statistics

A. The relationship between ζ_{g6} and ζ_{o6} .

The relationship between ζ_{g6} and ζ_{o6} is represented separately for winter and summer cases by scatter diagrams (figs. 8 and 9). Table 5 summarizes the following statistics: the number of cases, n , the arithmetic means, $\bar{\zeta}_{g6}$ and $\bar{\zeta}_{o6}$; the standard deviations, σ_{g6} and σ_{o6} ; the linear correlation coefficients, r ; the standard error of estimating ζ_{g6} from ζ_{o6} , S_{g6} ; the standard error of estimating ζ_{o6} from ζ_{g6} , S_{o6} ; and the root mean square of the absolute differences between ζ_{o6} ,

ζ_{g6} , $\text{rms } \zeta_6$.

Table 5. Statistical summary of comparative analysis of 600 km geostrophic and observed vorticities.

Group	n	$\bar{\zeta}_{g6}$	$\bar{\zeta}_{o6}$	σ_{g6}	σ_{o6}	r	S_{g6}	S_{o6}	$\text{rms } \zeta_6$
Winter	141	0.97	-0.33	3.55	2.98	.764	2.28	1.92	2.65
Summer	244	1.16	-1.25	2.69	2.60	.653	2.04	1.97	3.26
Total	385	1.09	-0.91	3.03	2.78	.689	2.20	2.02	3.05

There is some evidence of a seasonal effect in the fact that for the summer group the correlation coefficient is somewhat lower, the spread of the means is slightly increased and the standard deviations of both vorticities are decreased. The standard error of estimating ζ_{g6} from ζ_{o6} is slightly lower for the summer group; the root mean square of the absolute differences is larger for the summer cases. If we consider all

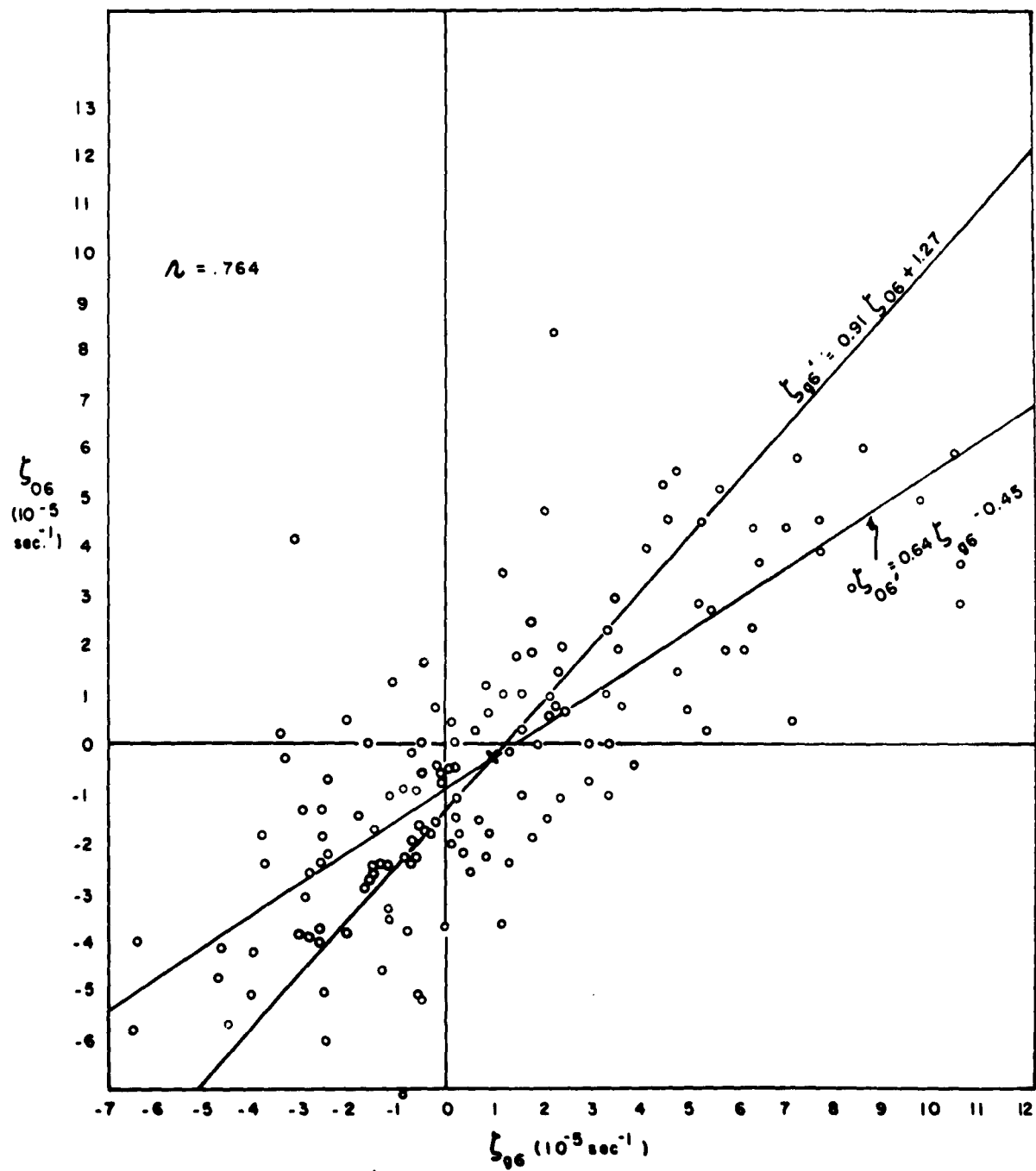


FIG. 8. Scatter diagram of ζ_{06} vs. ζ_{96} . Winter cases

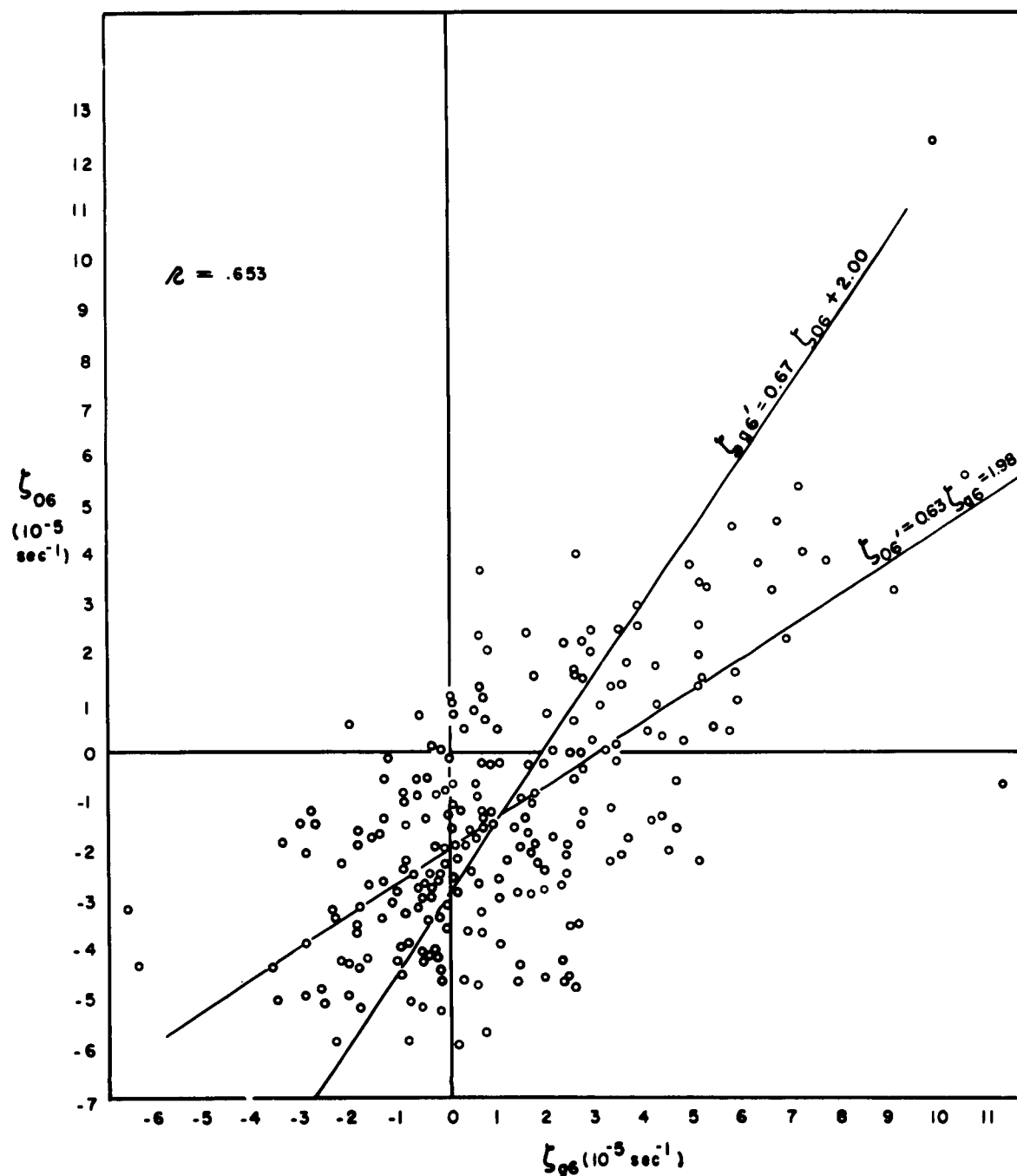


FIG. 9. Scatter diagram of ζ_{06} vs. ζ_{96} . Summer cases

the cases, the separation of the means of the vorticities is equal to slightly over 20 percent of the value of the Coriolis parameter; the standard errors of estimating one vorticity from the other is also about 20 percent of the Coriolis parameter; the root mean square of the absolute differences is over 30 percent of the value of the Coriolis parameter. The correlation coefficient for all the cases indicates that 47 percent of the variance of one vorticity can be accounted for by the other, --for the winter cases alone, 58 percent; for the summer cases alone, 43 percent. The following is a list of the equations of the regression lines:

1. All cases : $\zeta'_{g6} = 0.75 \zeta_{o6} + 1.77$
 $\zeta'_{o6} = 0.63 \zeta_{g6} - 1.60$
2. Winter cases : $\zeta'_{g6} = 0.91 \zeta_{o6} + 1.27$
 $\zeta'_{o6} = 0.64 \zeta_{g6} - 0.95$
3. Summer cases: $\zeta'_{g6} = 0.67 \zeta_{o6} + 2.00$
 $\zeta'_{o6} = 0.63 \zeta_{g6} - 1.98$

If we assume typical values of ζ_{o6} and use the regression equations given above to estimated values of ζ_{g6} , we obtain the values shown in Table 6.

Table 6. 600 km geostrophic vorticities estimated from regression equation for various values of 600 km observed vorticity.

$\zeta_{o6} \backslash \zeta'_{g6}$	winter	summer	all cases
-10	- 7.8	- 4.7	- 5.7
- 5	- 3.3	- 1.4	- 2.0
0	1.3	2.0	1.8
5	5.8	5.4	5.5
10	10.4	8.7	9.3
15	14.9	12.1	13.0

If we assume typical values of ζ_{g6} and similarly compute the estimated values of ζ_{o6} , we obtain the values shown in Table 7.

Table 7. 600 km "observed" vorticities estimated from regression equation for various values of 600 km geostrophic vorticity.

$\zeta_{g6} \backslash \zeta'_{g6}$	winter	summer	all cases
-10	- 7.4	- 8.3	- 7.9
- 5	- 4.2	- 5.1	- 4.8
0	- 1.0	- 2.0	- 1.6
5	2.2	1.2	1.6
10	5.4	4.3	4.7
15	8.6	7.5	7.8

B. The relationship between ζ_{g6} and ζ_{g3} .

The relation between ζ_{g6} and ζ_{g3} , the geostrophic vorticities on the two different scales, is represented for the separate groups of winter and summer cases by scatter diagrams (figs. 10 and 11). Table 8 represents statistics similar to those listed in Table 5 for ζ_{g6} and ζ_{g3} , where now S'_{g6} is the standard error of estimating ζ_{g6} from ζ_{g3} , and S_{g3} is the standard error of estimating ζ_{g3} from ζ_{g6} .

Table 8. Statistical summary of comparative analysis of 300 km and 600 km geostrophic vorticities.

Group	n	$\overline{\zeta_{g6}}$	$\overline{\zeta_{g3}}$	σ_{g6}	σ_{g3}	r	S'_{g6}	S_{g3}
Winter	141	0.92	5.52	3.55	7.16	.726	2.43	4.93
Summer	244	1.16	7.44	2.69	7.44	.740	1.81	5.01
Total	385	1.09	6.74	3.03	7.39	.723	2.09	5.11

The evidence of a seasonal effect is not as strong as was found in the study of ζ_{g6} and ζ_{06} . The correlation coefficients for the separate winter and summer cases show remarkable agreement; however, the spread of the means, as before, is greater for the summer group. The winter and summer values of σ_{g3} and S_{g3} are in close agreement. The standard error of estimating ζ_{g3} from ζ_{g6} is very large, approximately 55 percent of the value of the Coriolis parameter.

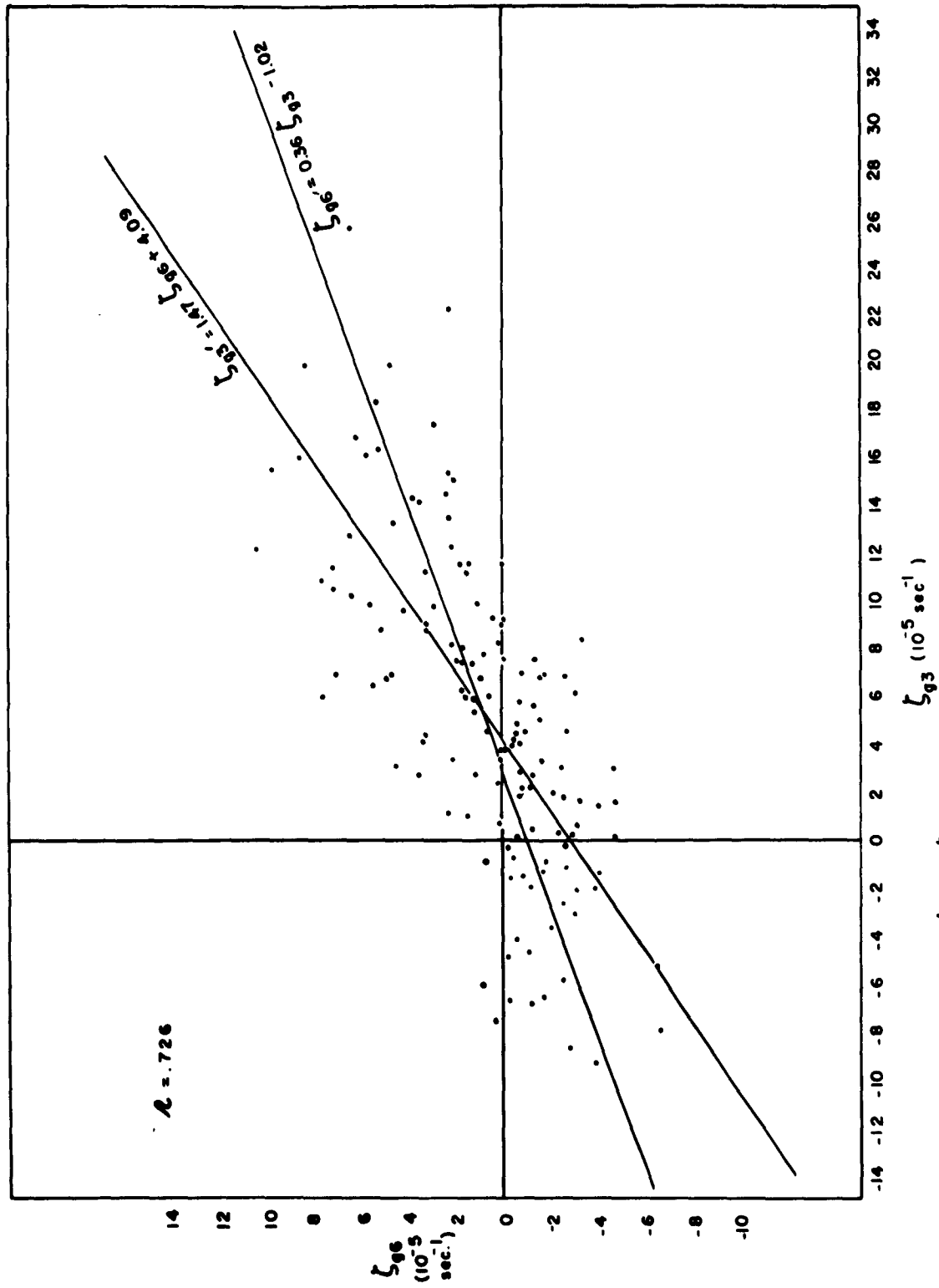


FIG. 10. Scatter diagram of L_{96} vs. L_{93} . Winter cases.

15

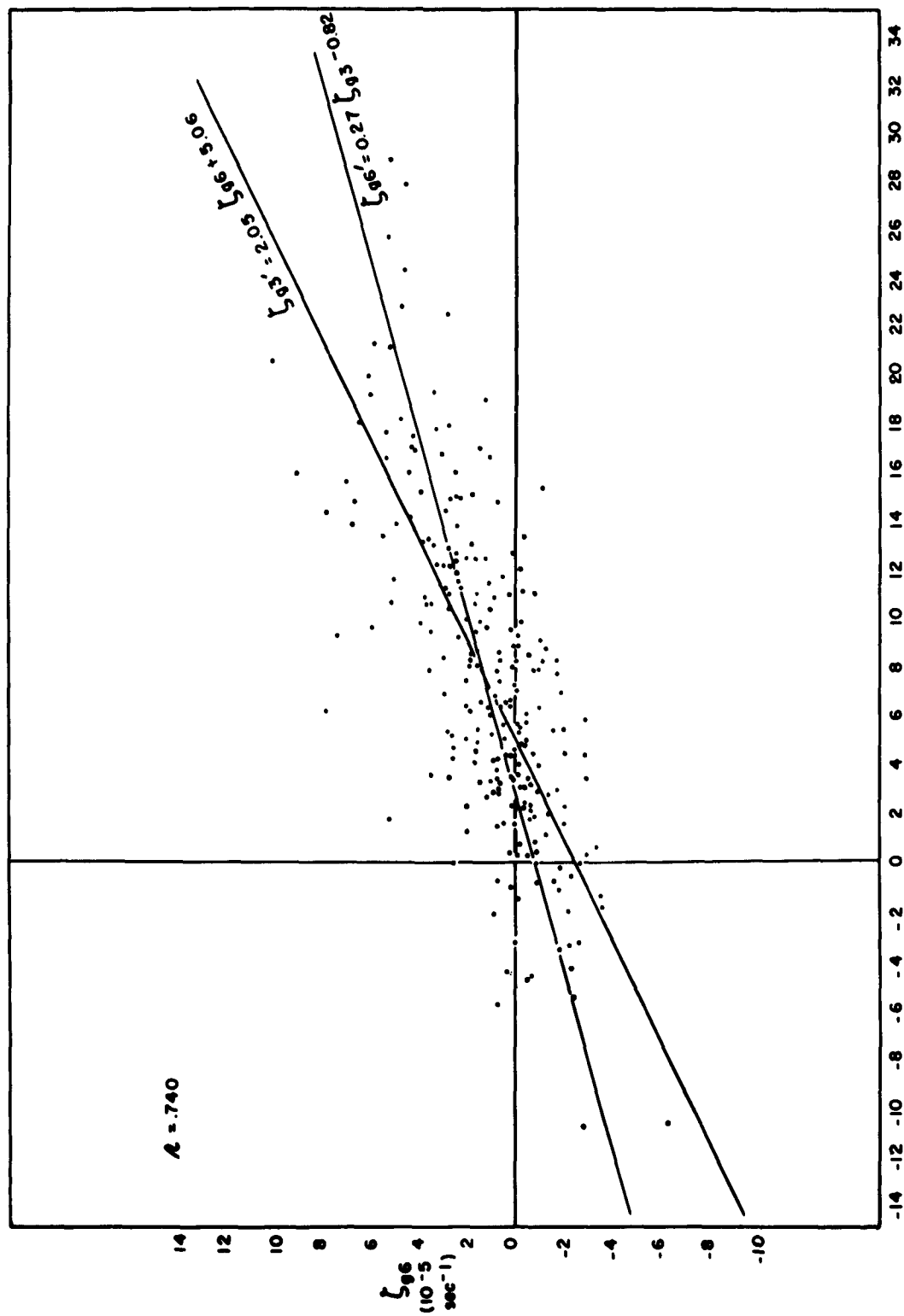


FIG. 11. Scatter diagram of L_{96} vs. L_{93} . Summer cases.

If we consider all the cases, the differences in the means and the standard deviations are quite striking. Yet, the two vorticities are rather highly correlated, since 52 percent of the variance of one can be accounted for by the other. The following is a list of the equations of the regression lines:

1. All cases : $\zeta'_{g6} = 0.30 \zeta_{g3} - 0.91$
 $\zeta'_{g3} = 1.76 \zeta_{g6} + 4.82$
2. Winter cases : $\zeta'_{g6} = 0.36 \zeta_{g3} - 1.02$
 $\zeta'_{g3} = 1.47 \zeta_{g6} + 4.09$
3. Summer cases: $\zeta'_{g6} = 0.27 \zeta_{g3} - 0.82$
 $\zeta'_{g3} = 2.05 \zeta_{g6} + 5.06$

If we assume typical values of ζ_{g3} and use the regression equations as given above to compute the estimated values of ζ_{g6} , we obtain the values shown in Table 9.

If we assume typical values of ζ_{g6} and compute the estimated values of ζ_{g3} , we obtain the values in Table 10.

If one were to assume a linear variation of the height differences, $(h_1 - h_0)$, etc., from one grid scale to another, one would expect a given value of ζ_{g6} to be one-half that of the corresponding value of ζ_{g3} , since the computation of geostrophic vorticity depends inversely upon L^2 , the square of the grid differentiation distance. It would appear, from the sample calculations made from the regression equations, that the use of positive values of ζ_{g3} to calculate ζ_{g6} produces an estimate of the

Table 9. 600 km geostrophic vorticities estimated from regression equation for various values of 300 km geostrophic vorticity.

$\xi_{g3} \backslash \xi'_{g6}$	Winter	Summer	All cases
-10	- 4.6	- 3.5	- 3.9
- 5	- 2.8	- 2.2	- 2.4
0	- 1.0	- 0.8	- 0.9
5	0.8	0.5	0.6
10	2.6	1.9	2.1
15	4.4	3.2	3.6
20	6.2	4.6	5.1
25	8.0	5.9	6.6
30	9.8	7.3	8.1

Table 10. 300 km geostrophic vorticities estimated from regression equation for various values of 600 km geostrophic vorticity.

$\xi_{g6} \backslash \xi'_{g3}$	Winter	Summer	All cases
-10	-10.6	-15.4	-12.8
- 5	- 3.3	- 5.2	- 4.0
0	4.1	5.1	4.8
5	11.4	15.3	13.6
10	18.8	25.6	22.4
15	26.1	35.8	31.2

larger-scale geostrophic vorticity considerably less than one-half the value of the smaller-scale vorticity. On the other hand, the use of ζ_{g6} to estimate ζ_{g3} produces values of the smaller-scale vorticity which are, generally speaking, about twice that of the larger-scale vorticity.

4. Discussion of Errors and Unrepresentativeness

Before attempting a final evaluation of the statistical results, an estimate should first be made of the variance introduced into the calculations by errors in the measurement of heights and winds and by small-scale fluctuations. We shall consider here the error standard deviation. From equation (3), it is obvious that the calculation of geostrophic vorticity is most sensitive to errors in measuring the height of the central station. The error standard deviation of the geostrophic vorticities can be shown (Scarborough, 1930) to be

$$\hat{\sigma}_{\zeta_g} = \sqrt{\left(\frac{\partial \zeta_g}{\partial h_1}\right)^2 \sigma_{h1}^2 + \left(\frac{\partial \zeta_g}{\partial h_2}\right)^2 \sigma_{h2}^2 + \left(\frac{\partial \zeta_g}{\partial h_3}\right)^2 \sigma_{h3}^2 + \left(\frac{\partial \zeta_g}{\partial h_4}\right)^2 \sigma_{h4}^2 + \left(\frac{\partial \zeta_g}{\partial h_o}\right)^2 \sigma_{ho}^2} \quad (4)$$

If we assume that the error variances of the height values are equal for the five stations, we obtain, after simplifying

$$\hat{\sigma}_{\zeta_g} = \frac{\sqrt{20} \sigma_h g}{fL^2} \quad (5)$$

If we now use Rapp's (1952) estimate of the error variance of the height of the 500 mb surface, $\sigma_h^2 = 104.5 \text{ m}^2$, we obtain as the error

standard deviation of ζ_{g3} ,

$$\hat{\sigma}_{\zeta_{g3}} = 5.2 \times 10^{-5} \text{ sec}^{-1}.$$

Similarly, we obtain as the error standard deviation of ζ_{g6} ,

$$\hat{\sigma}_{\zeta_{g6}} = 1.3 \times 10^{-5} \text{ sec}^{-1},$$

a value one-fourth that of $\hat{\sigma}_{\zeta_{g3}}$.

If we now also consider equation (1) used in computing the observed vorticity, we can express the error standard deviation of the observed vorticity as

$$\hat{\sigma}_{\zeta_o} = \sqrt{\left(\frac{\partial \zeta_o}{\partial v_3}\right)^2 \sigma_{v3}^2 + \left(\frac{\partial \zeta_o}{\partial v_1}\right)^2 \sigma_{v1}^2 + \left(\frac{\partial \zeta_o}{\partial u_2}\right)^2 \sigma_{u2}^2 + \left(\frac{\partial \zeta_o}{\partial u_4}\right)^2 \sigma_{u4}^2} \quad (6)$$

If we assume that $\sigma_{v3}^2 = \sigma_{v1}^2$ and $\sigma_{u2}^2 = \sigma_{u4}^2$, it can be shown that

$$\hat{\sigma}_{\zeta_o} = \frac{\sqrt{2}}{L} \sqrt{\sigma_v^2 + \sigma_u^2} \quad (7)$$

From Rapp's results the average error variances of the east-west and north-south wind components between 5.5 and 6.0 km above sea level (the approximate range of the height of the 500 mb surface) are found to be $\sigma_u^2 = .65 \text{ m}^2 \text{ sec}^{-2}$ and $\sigma_v^2 = .79 \text{ m}^2 \text{ sec}^{-2}$. Thus the error standard deviation of ζ_{o6} is found to be

$$\hat{\sigma}_{\zeta_{o6}} = .24 \times 10^{-5} \text{ sec}^{-1}.$$

These estimates of the error standard deviations must be viewed, however, as being on the low side, since Rapp's statistical values were based upon data more accurate than that obtained in daily observational routine.

In addition to the variance produced by errors in measuring heights and winds, the variance of small-scale fluctuations should be considered. It is probable that this variance is of considerable importance, since the wind observations are, in effect, non-simultaneous, and the small-scale fluctuations are of a short enough period (5 minutes to 3 hours) to seriously affect vorticity computations based on the reported winds of five stations.

Rapp lists as possibly useful approximations to the average magnitudes of the variances of the small-scale fluctuations, values of $\hat{\sigma}_u^2$ and $\hat{\sigma}_v^2$, for various heights as determined from four separate experiments. The values which he obtained for $\hat{\sigma}_u^2$ and $\hat{\sigma}_v^2$, between 5 and 6 km were then averaged. The mean of seven values of $\hat{\sigma}_u^2$ was $3.3 \text{ m}^2 \text{ sec}^{-2}$; the mean of five values of $\hat{\sigma}_v^2$ was $10.1 \text{ m}^2 \text{ sec}^{-2}$ (due to the occurrence of two values exceeding $20 \text{ m}^2 \text{ sec}^{-2}$). If we assume that $\hat{\sigma}_u^2$ and $\hat{\sigma}_v^2$ are each equal to a value of approximately $5 \text{ m}^2 \text{ sec}^{-2}$, the standard deviation of the observed vorticity produced by small-scale wind fluctuations is

$$\hat{\sigma}_{\text{go6}} = 1.7 \times 10^{-5} \text{ sec}^{-1}.$$

The above values of the standard deviations of vorticity resulting from observational error and small-scale fluctuations are proposed as rough qualitative estimates. It would seem reasonable, however, to assume that the variance of observed vorticity due to small-scale wind fluctuations significantly exceeds that due to errors in wind measurement,

and that their combined variance is comparable to that of the geostrophic vorticity of the same scale.

5. Conclusions

On the basis of the results of this study, it is concluded that geostrophic and observed relative vorticity, when measured on the same scale of 600 km, are closely related, especially during the winter. In the "winter" months 58 percent of the variance of one vorticity can be accounted for by the other; in the "summer" months only 43 percent can be accounted for. No great disparity could be found in the standard deviations or in the standard error of estimating one vorticity from the other, except for a slight tendency for $\sigma_{\xi_{g6}}$ to be larger than $\sigma_{\xi_{o6}}$, an effect more pronounced in the winter cases. The geostrophic and observed vorticities, although closely related, are not identical in magnitude. The root mean square values of the absolute differences $|\xi_{g6} - \xi_{o6}|$ indicate rather significant differences in their magnitudes, even if we consider the effect of observational errors and unrepresentativeness. The standard error of estimating one vorticity from the other is considerable, about 20 percent of the value of the Coriolis parameter (for the region of study, $f \approx 9 \times 10^{-5} \text{ sec}^{-1}$). If we consider, moreover, the variance of small-scale wind deviations in addition to the error variance of wind measurement, it is probable that observed vorticity cannot be more accurately measured than the geostrophic vorticity.

The results of the study of 300 km and 600 km geostrophic vorticity indicate the important effect of grid size upon geostrophic computations. This effect is mainly brought about by second order differentiation of the height field, so that even with a linear variation of height differences, doubling the grid size reduces the relative vorticity by one-half. The results seem to show that the vorticity centers are of such small scale that doubling the grid size from 300 km to 600 km will reduce the values of vorticity even further. The effect produced by errors in height measurement upon the computation of geostrophic vorticity is also dependent on scale since the effect of doubling the grid size is to reduce error variance to one-fourth that of the smaller scale.

The first study of ζ_{06} and ζ_{g3} failed because it was based upon a fallacious assumption that vorticities of different scales were comparable. The scale of measurement has such an important effect upon the computation of geostrophic vorticity, that it might also be expected to have a similar effect upon observed vorticity, although this effect could not be directly evaluated in this study.

Acknowledgment

The writer wishes to express his thanks to Professor Jerome Spar for his continued guidance, assistance and encouragement during the course of this study.

References

- Aubert, E. J., 1953: The correspondence between relative vorticity of the observed and geostrophic winds. G.R.D., Air Force Cambridge Research center (unpublished).
- Charney, J. G., 1948: On the scale of atmospheric motions. Geophys. Publ., vol. 17, no. 2, pp. 1-17.
- Godson, W. L., 1950: A study of the deviation of wind speeds and directions from geostrophic values. Q. J. R. M. S., 76: 3-15.
- Houghton, H. G., and J. M. Austin, 1946: A study of non-geostrophic flow with applications to the mechanism of pressure changes. J. of Meteor. 3: 57-77.
- Hovmöller, E., 1952: A comparison between observed and computed winds with respect to their applicability for vorticity computations. Tellus, 4: 126-134.
- Landers, H., 1955: Analysis of some "Project Jet Stream" data. BAMS, 36: 371-378.
- Miller, J. E., 1947: Non-geostrophic flow and the mechanism of pressure change (letter). J. of Meteor., 4: 72.
- Neiburger, M., et al., 1948: On the computation of wind from pressure data. J. of Meteor., 5: 87-92.
- Newton, 1954: Analysis and data problems in relation to numerical prediction. BAMS, 35: 287-294.
- Rapp, R. R., 1952: The effect of variability and instrumental error on measurements in the free atmosphere. Meteorological Papers, vol. 2, no. 1, New York University.
- Reed, R. J., 1951: A study of atmospheric vorticity. Technical Report No. 10, Research on Atmospheric Pressure Changes, M. I. T.
- Scarborough, J. B., 1930: Numerical Mathematical Analysis. The Johns Hopkins Press, Baltimore, 416 pp.
- Spar, J., E. L. Fisher, E. Paroczay, and R. E. Peterson, 1955: Vorticity changes in an east coastal cyclone. Progress Report No. 2, Project SCUD, Contract No. Nonr 285(09), New York University.